Serviceability of masonry arch railway bridges

T.M. Roberts and T.G. Hughes
Cardiff University, School of Engineering, Cardiff, Wales, UK

ABSTRACT: Site monitoring of an existing masonry arch railway bridge, with a view to obtaining qualitative and quantitative information concerning deflections, transverse load distribution and differential longitudinal movements that may exacerbate the longitudinal cracking observed in many such bridges, is described. The monitoring was undertaken using eight accelerometers attached to the underside of the bridge. Low frequency drift in the integrated displacements was suppressed in the time domain using developed numerical procedures. Due to longitudinal cracking the bridge behaved as two distinctly separate arches, with negligible transverse load distribution. Recorded accelerations and processed displacements clearly indicated the response of the bridge to loading transmitted via individual bogies, while the response to individual axle loads was less apparent.

1 INTRODUCTION

Masonry arch bridges continue to play an important role in the transport infrastructure of the UK, forming a significant proportion of road, rail and waterway crossings. Many of these bridges are relatively old and are being subjected to increasing demands in terms of vehicle numbers, loads and speeds. While the majority of experimental and theoretical investigations to date have been concerned primarily with the determination of ultimate or failure loads, the need to establish serviceability limits for such structures, to safeguard against progressive damage and ensure that they continue to perform in a satisfactory manner, has also been recognized (Boothby et al. 1998, Harvey 1991, 2006, Hughes and Blackler 1997).

Previous studies at Cardiff University, undertaken on behalf of Network Rail, have been directed towards establishing high cycle fatigue strength curves for brick masonry subjected to concentric and eccentric loading (Roberts et al. 2006). While in general fatigue strength curves can be used to predict the fatigue life of structures there are many uncertainties in attempting to predict the remaining fatigue lives of existing masonry arch bridges. Since many such bridges are more than 100 years old construction details and the strength and stiffness of the materials are subject to significant variation, and are difficult to assess without damaging the structure. Dynamic effects related to train velocity, impact and oscillations can result in significant amplification of deflections and induced stresses. Also masonry arch bridges are highly heterogeneous three dimensional structures, the behavior of which is influenced by long term movements affecting in situ stresses, ring separation and other forms of cracking, environmental effects etc. For such structures even the most sophisticated three dimensional methods of analysis are likely to be unreliable.

The aims of the present study were to monitor the dynamic response of an existing masonry arch railway bridge, with a view to obtaining qualitative and quantitative information concern

ing deflections, transverse load distribution, and differential longitudinal movements that may be the cause of the longitudinal cracking observed in many such bridges.

2 SITE MONITORING AND DATA PROCESSING

2.1 Bridge details

Dinmore masonry arch railway under bridge is situated at Hope under Dinmore, approximately mid way between Hereford and Leomster, at grid reference SO 508 529. The bridge was constructed circa 1853 and is a semi circular, stone faced, brick masonry arch, with a clear span of 3.6 m, a maximum soffit height of 3.9 m and a width of 8.6 m (see Fig. 1). The bridge carries two railway tracks over a narrow country lane, approximately 3.5 m wide. Cores taken in the year 2000 indicated the brick masonry arch barrel to be approximately 500 mm thick.

Figure 1 : Dinmore Parsons Farm brick masonry arch railway under bridge.

2.2 Data acquisition system

A diagrammatic representation of the data acquisition system, supplied by the National Instruments Corporation (UK), is shown in Fig. 2. The SCXI system hardware comprised the following components.

- SCXI-1000 chassis energized by a 110 to 240 volt AC power supply
- SCXI-1540 eight channel LVDT signal conditioning module
- SCXI-1315 terminal block for connecting up to eight LVDTs
- SCXI-1520 eight channel deluxe bridge with excitation
- SCXI-1314 terminal block for connecting up to eight accelerometers
- SCXI-1600 USB digitizer module capable of sampling analogue signals from the LVDT conditioner and accelerometer bridge at a frequency of 200 000 samples per second, connected via a USB cable to a Samsung X05 Plus 715 notebook.
- LVDTs Type D5/400AG with an operating range of ±10 mm.
- Accelerometers Type 060-F482-02 with an operating range of ±5 g.

The LVDTs and accelerometers were supplied by RDP Electronics Ltd. The LVDTs were calibrated using a micrometer calibration device reading to an accuracy of 0.001 mm. The accelerometers were calibrated using a so called flip test i.e. the readings were adjusted to register a difference of 2 g when the accelerometer was rotated through 180^{o} in a vertical plane, from

the axis up position to the axis down position. It was observed that the accelerometers so calibrated did not register exactly the mean of the axis up and axis down readings when the axis was horizontal.

The system was controlled by a bespoke LabVIEW program stored in the Samsung notebook. The LabVIEW program comprised a main program for controlling operation and saving data, a calibration sub program for calibrating and initializing output signals from the LVDTs and accelerometers, and a trigger sub program for triggering the system in response to a pre defined signal amplitude from one of the LVDTs.

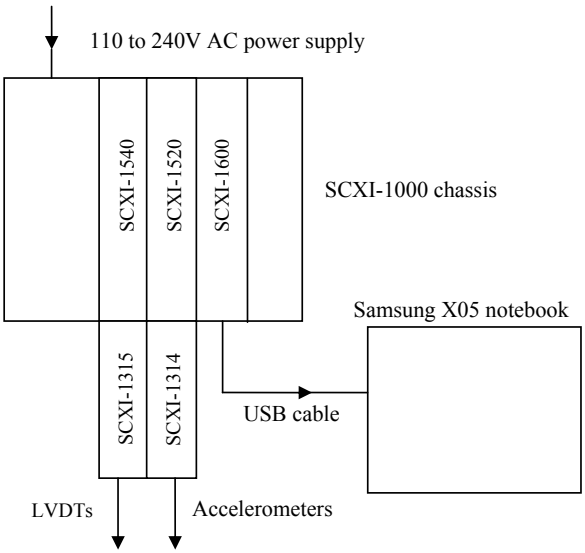

Figure 2 : Diagrammatic representation of data acquisition system.

2.3 Site monitoring

Initially it was planned to monitor the bridge using both the LVDTs and accelerometers. Monitoring with the LVDTs would have required the erection of a reaction frame beneath the bridge, necessitating temporary closure of the road. Since this was not permitted monitoring was carried out using only the accelerometers.

Eight accelerometers were attached to the underside of the bridge using aluminum mounting blocks. Karabiner type spring hooks, attached to the mounting blocks, enabled the gauge extension cables to be attached securely to the underside of the bridge. The recording equipment was located in a vehicle parked in a small lay bye about 30 m east of the bridge, and was powered by a 110 volt AC generator.

The accelerometers were positioned on the underside of the bridge as shown in Fig. 3. All of the accelerometers, except 2 and 6, were orientated to measure the radial acceleration of the arch barrel. Accelerometers 2 and 6 were placed beneath the crown and orientated to measure the tangential acceleration of the arch barrel.

2.4 Data processing

Double integration of the acceleration data, to give velocity and displacement, was performed using an Excel spreadsheet based on a simple trapezoidal formula represented by the equation

$$\int_{t_i}^{t_{i+1}} X(t)\,dt = \{X(t_i) + X(t_{i+1})\}\frac{\Delta t}{2} \qquad (1)$$

where t = time, Δt = sampling interval and X(t) = the integrand. However, the integrated displacements exhibited unacceptable low frequency drift. This drift could not be eliminated either

by increasing the sampling frequency (up to 1000 sps) or by using a more accurate cubic integration formula. It was concluded that the low frequency drift was due to very small biased errors in the accelerometer readings. Conversion of the accelerometer readings from g = 9.81 m/sec^2 to mm/sec^2 and integrating twice over a ten second period has the effect of magnifying a biased error by 10^6. It was further concluded that the only option was to filter the low frequency drift numerically.

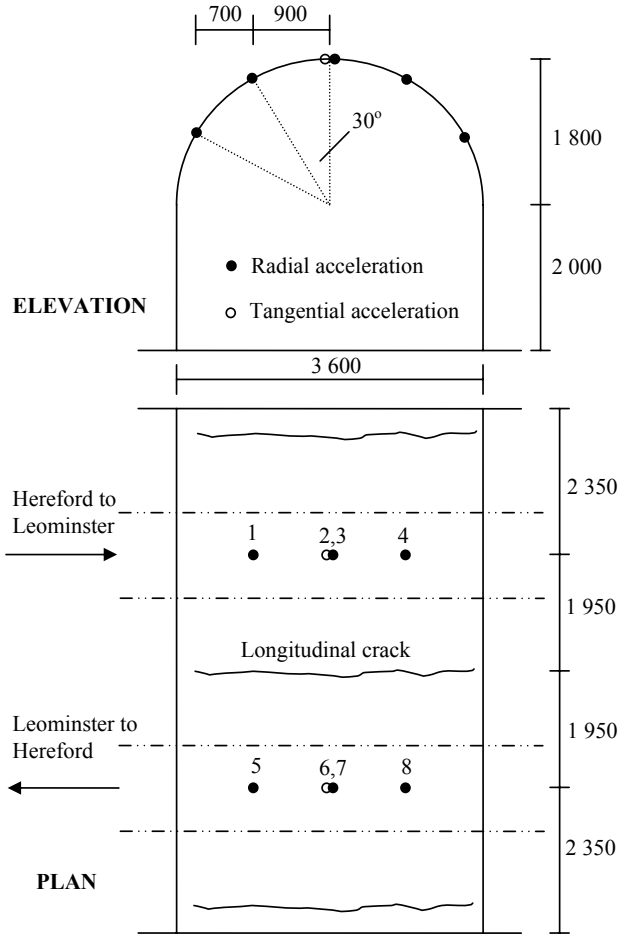

Figure 3 : Location and numbering of accelerometers.

It was assumed that the dynamic response of a system X(t) could be represented by an infinite series of terms in the form

$$X(t) = \sum_{m=1}^{\infty} X_m(t) = \sum_{m=1}^{\infty} X_m \sin m\omega t = \sum_{m=1}^{\infty} X_m \sin \frac{2\pi}{T_m} t \qquad (2)$$

where ω = a reference circular frequency, X_m = maximum amplitude corresponding to circular frequency $m\omega$ (rads per sec) and period T_m (secs). The average value of $X_m(t)$ over all periods T_n for which m is an integer multiple of n is zero. The average value of $X_m(t)$ when $m < n$ will not however be zero.

Low frequency amplitude suppression can therefore be effected by reducing all values of X(t) by the average value of X(t) over the time interval $t - \Delta T_n / 2$ to $t + \Delta T_n / 2$. For $m / n = 0.5$ values of $X_m(t)$ are effectively multiplied by a reduction factor having a minimum value of $(1 - 2 / \pi) = 0.36$. This factor rapidly approaches zero as m / n becomes small. Care should be exercised if the dynamic response has components for which m is not an integer multiple of n. For $m / n = 1.5$ the minimum value of the reduction factor is $(1 - 2 / 3\pi) = 0.79$. This factor rapidly approaches 1 as m increases.

The effectiveness of the numerical procedure for filtering low frequency drift is illustrated in Fig. 4, which shows the results of a laboratory test on a vibrating steel cantilever beam. The displacement and acceleration of a point close to the end of the beam were measured using a LVDT and an accelerometer respectively.

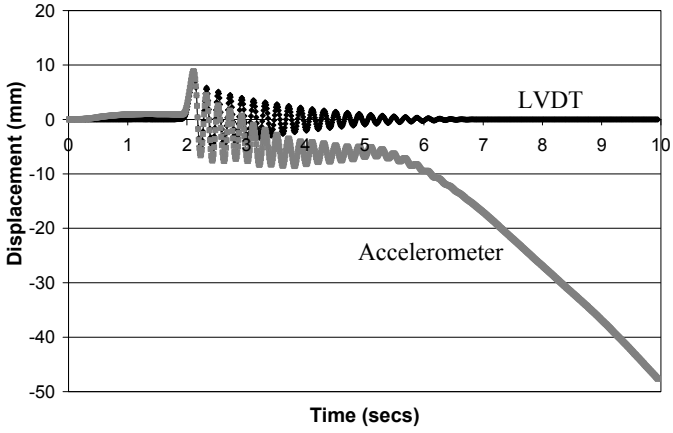

(a) Results without low frequency amplitude filtering

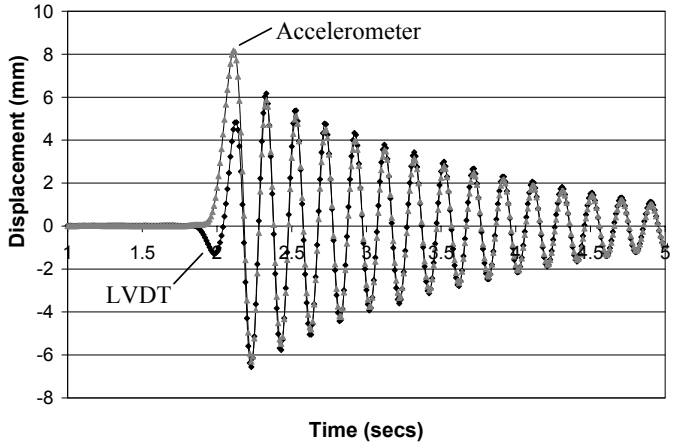

(b) Results with low frequency amplitude filtering

Figure 4 : Comparison of LVDT and integrated accelerometer displacements for a vibrating cantilever beam.

3 TEST RESULTS

3.1 General

For each test the LVDT trigger was activated manually. Accelerometer readings were recorded for a period of about ten seconds, including a pre trigger period of about four seconds to record the ambient accelerometer readings. The sampling frequency for all tests was 1000 sps.

Prior to integration the accelerometer readings were reduced to a zero datum by subtracting the average of the pre trigger ambient readings. Low frequency filtering was then applied to the integrated displacements (below 5 Hz for accelerometers 2 and 6 and below 2.5 Hz for all other accelerometers).

3.2 Test M1-TMV-LH

Test results for a track maintenance vehicle traveling on the Leominster to Hereford line are presented in Figs. 5 and 6.

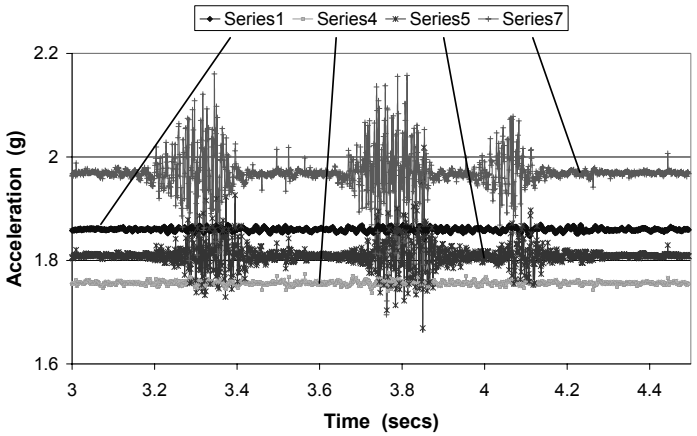

Figure 5 : Recorded accelerations for test M1-TMV-LH.

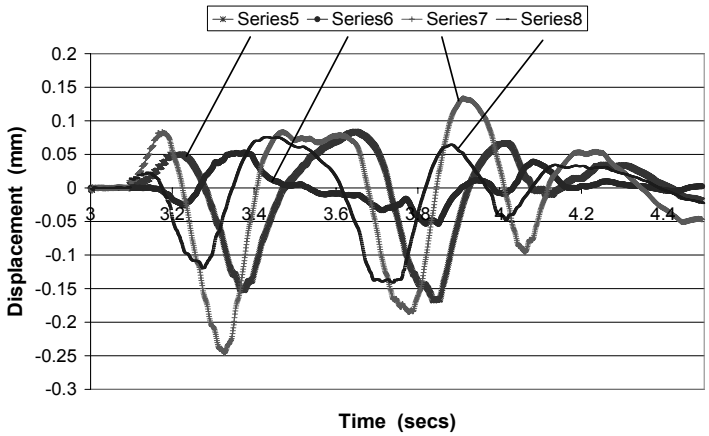

Figure 6 : Integrated displacements for test M1-TMV-LH.

Figure 5 shows the recorded readings from accelerometers 1, 4, 5 and 7 (series 1, 4, 5 and 7). Accelerometers 1 to 4 did not register any response while accelerometers 5 to 8 registered a sig-

nificant response to three bogies as the vehicle crossed the bridge. It appears therefore that the longitudinal cracking of the bridge, indicated in Fig. 3, resulted in the bridge behaving as two distinctly separate arches.

Figure 6 shows the integrated displacements, with low frequency amplitude filtering, for accelerometers 5 to 8. The results exhibit a relatively small positive shift from the axis of zero displacement due to the low frequency filtering. The most reliable estimate of the displacement amplitude is therefore the peak to peak amplitude.

The results presented in Fig. 6 indicate the passage of three bogies over the bridge, two of approximately equal weight followed by a third of approximately half the weight. There is little evidence of a bridge response to individual axle loads. The maximum radial and tangential displacements at the crown were approximately 0.35 mm and 0.04 mm respectively.

While in general there are small residual errors in the processed results, after the low frequency filtering, the results as presented provide good qualitative and reasonable quantitative indications of the response of the bridge to the passing train.

3.3 Test M5-FT-LH

Test results for a freight train traveling on the Leominster to Hereford line are presented in Fig. 7. Accelerometers on the Hereford to Leominster line did not register any significant response. The results indicate the passage of two heavily loaded bogies followed by a succession of lightly loaded bogies, indicating that the wagons were probably empty (confirmed by the Area Maintenance Engineer).

The maximum radial and tangential displacements at the crown were approximately 0.7 mm and 0.15 mm respectively.

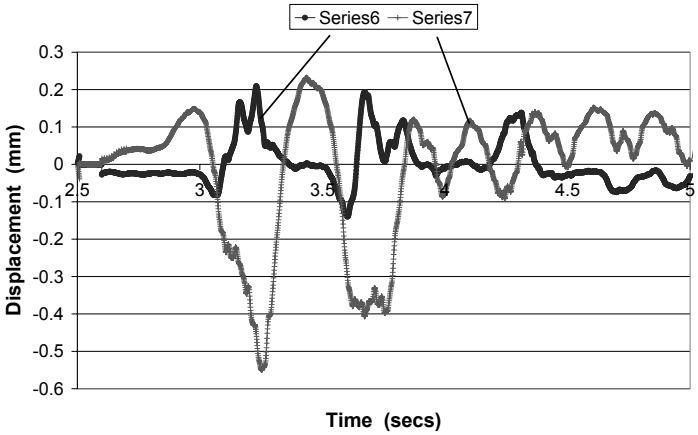

Figure 7 : Integrated displacements for test M5-FT-LH.

3.4 Test M7-PT2-HL

Test results for a two coach passenger train traveling on the Hereford to Leominster line are presented in Fig. 8. Accelerometers on the Leominster to Hereford line did not register any response. The results indicate the passage of four bogies, two closely spaced where the coaches were connected and two more widely spaced at each end of the train. The maximum radial and tangential (not shown for clarity) displacements at the crown were approximately 0.5 mm. and 0.1 mm respectively.

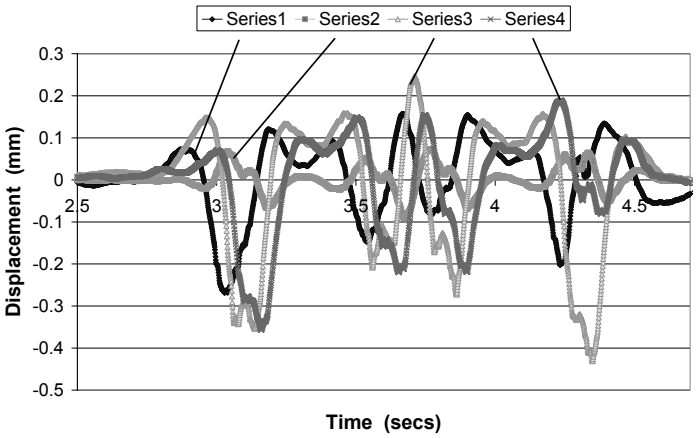

Figure 8 : Integrated displacements for test M7-PT2-HL.

4 DISCUSSION AND CONCLUSIONS

Site monitoring of Dinmore Parsons Farm masonry arch railway under bridge was carried out using eight accelerometers attached to the underside of the bridge. The following conclusions can be drawn from the recorded and processed test results.

Due to longitudinal cracking the bridge behaved as two distinctly separate masonry arches.

Recorded accelerations and processed displacements clearly indicated the response of the bridge to loading transmitted via individual bogies. The response of the bridge to individual axle loads was much less apparent.

The maximum recorded radial and tangential displacements at the crown were approximately 0.7 mm and 0.25 mm respectively.

The integrated displacements, with low frequency amplitude filtering, exhibit small residual errors, which have been estimated to be less than 10% of the maximum displacement.

ACKNOWLEDGEMENT

The work described herein was sponsored by Network Rail, under the supervision of Mr Brian Bell, whose financial and technical support is gratefully acknowledged.

REFERENCES

Boothby, T. E., Domalik, D. E. and Dalal, V. A. 1998. Service load response of masonry arch bridges. *Journal of Structural Engineering, ASCE*, 124(1), p. 17-23.

Harvey, W. J. 1991. Stability strength elasticity and thrust lines in masonry arches. *The Structural Engi neer*, 69(9), p. 181-184.

Harvey, W. J. 2006. Some problems with arch bridge assessment and potential solutions. *The Structural Engineer*, 84(3), p. 45-50.

Hughes, T. G. and Blackler, M. J. 1997. A review of the UK masonry arch assessment methods. *Proc. ICE, Structures and Buildings*, 122, p. 305-315.

Roberts, T. M., Hughes, T. G., Dandamudi, V. R. and Bell, B. 2006. Quasi static and high cycle fatigue strength of brick masonry. *Construction and Building Materials*, 20(9), p.603-614.